

The rise of 2D materials/ferroelectrics for next generation photonics and optoelectronics devices

Cite as: APL Mater. 10, 060903 (2022); <https://doi.org/10.1063/5.0094965>

Submitted: 07 April 2022 • Accepted: 27 May 2022 • Published Online: 24 June 2022

 Linghua Jin, Huide Wang, Rui Cao, et al.



View Online



Export Citation



CrossMark

ARTICLES YOU MAY BE INTERESTED IN

[Ferroelectric field effect transistors: Progress and perspective](#)

APL Materials **9**, 021102 (2021); <https://doi.org/10.1063/5.0035515>

[Next generation ferroelectric materials for semiconductor process integration and their applications](#)

Journal of Applied Physics **129**, 100901 (2021); <https://doi.org/10.1063/5.0037617>

[Empowering 2D nanoelectronics via ferroelectricity](#)

Applied Physics Letters **117**, 080503 (2020); <https://doi.org/10.1063/5.0019555>



Characterizing nanostructures?
Learn about a new way to get
high-quality data in a fraction of the time

Read the tech note

Lake Shore
CRYOTRONICS

The rise of 2D materials/ferroelectrics for next generation photonics and optoelectronics devices

Cite as: *APL Mater.* **10**, 060903 (2022); doi: [10.1063/5.0094965](https://doi.org/10.1063/5.0094965)

Submitted: 7 April 2022 • Accepted: 27 May 2022 •

Published Online: 24 June 2022



View Online



Export Citation



CrossMark

Linghua Jin,¹  Huide Wang,² Rui Cao,² Karim Khan,^{2,3}  Ayesha Khan Tareen,⁴ Swelm Wageh,⁵ 
Ahmed A. Al-Ghamdi,⁵ Shaojuan Li,⁶ Dabing Li,⁷  Ye Zhang,^{1,a)} and Han Zhang^{2,a)} 

AFFILIATIONS

¹School of Chemistry and Chemical Engineering, University of South China, Hengyang, Hunan 421001, China

²Shenzhen Engineering Laboratory of Phosphorene and Optoelectronics, College of Physics and Optoelectronic Engineering, Shenzhen University, Shenzhen 518060, China

³School of Electrical Engineering and Intelligentization, Dongguan University of Technology, Dongguan 523808, China

⁴School of Mechanical Engineering, Dongguan University of Technology, Dongguan 523808, China

⁵Department of Physics, Faculty of Science, King Abdulaziz University, Jeddah 21589, Saudi Arabia

⁶State Key Laboratory of Applied Optics, Changchun Institute of Optics Fine Mechanics and Physics, Chinese Academy of Sciences, Changchun 130033, China

⁷State Key Laboratory of Luminescence and Applications, Changchun Institute of Optics Fine Mechanics and Physics, Chinese Academy of Sciences, Changchun 130033, China

^{a)}Authors to whom correspondence should be addressed: yezhang@usc.edu.cn and h Zhang@usc.edu.cn

ABSTRACT

Photonic and optoelectronic devices have been limited in most two-dimensional (2D) materials. Researchers have attempted diverse device structures, such as introducing some ferroelectric materials to form new hybrid materials that could improve the performance of these 2D devices. Ferroelectrics might adjust the carrier concentration, mobility, and bandgap of 2D materials to achieve non-volatile control of the photonic and optoelectronic properties. On the other hand, ferroelectrics have a spontaneous electric polarization that occurs below the Curie temperature and reverses under an applied electric field. The polarization can be modulated via incident light, while the light wavelengths can be tuned through switching the electric polarization. This could improve the performance of 2D photonic and optoelectronic devices. We believe that 2D materials, as an emerging member of 2D/ferroelectric hybrid materials, will have great potential in photonics and optoelectronics thanks to their tunable bandgap. Here, we provide a perspective of ferroelectrics on 2D materials for photonics and optoelectronics. We discuss the concept of ferroelectrics and their fundamentals and then present their unique advantages in optoelectronic devices.

© 2022 Author(s). All article content, except where otherwise noted, is licensed under a Creative Commons Attribution (CC BY) license (<http://creativecommons.org/licenses/by/4.0/>). <https://doi.org/10.1063/5.0094965>

I. INTRODUCTION

Since Geim successfully prepared graphene through mechanical exfoliation in 2004, two-dimensional (2D) materials formed with weak interlayer van der Waals forces and strong intralayer covalent bonds have attracted widespread attention.^{1,2} The most noticeable among these 2D materials are transition metal sulfides (TMDs), graphene, black phosphorus (BP), and MXenes.^{3–9} In recent years, search on 2D materials has dramatically increased with the efforts

of many researchers, and they have become a research hotspot worldwide.

Unlike their bulk parents, 2D materials exhibit unique photonic and optoelectronic properties due to their diverse electronic structures and bandgap structures. Several of the 2D materials with abundant bandgaps ranging from 0 to several eV provide ultra-broadband light–matter interactions from deep ultraviolet to microwave.^{10–17} In addition, the radiative recombination lifetime between electrons and holes and the optoelectronic response can

be affected by the reduced dimensionality and associated reduced dielectric screening effects of 2D materials.¹⁸ Moreover, the characteristics of 2D materials without surface dangling bonds and the atomic thickness make it easier to be integrated with any substrate through van der Waals forces without lattice matching, suggesting the facile realization of multi-functional photonic and optoelectronic devices, including photoemitters, photodetectors, optical modulators, sensors, and nonlinear optical devices,^{19–35} as shown in Fig. 1. Therefore, 2D materials become a main stream trend in photonics and optoelectronics.

Despite providing access to novel photonic and optoelectronic devices, the limited spectral range or relative weak light absorption and the short interaction length between light and matter cannot be ignored. Thereby, the ability of photonic and optoelectronic devices has been limited in most 2D materials.^{19,36,37} To address these issues, many researchers in related fields have attempted diverse device structures, such as introducing some other smart materials to form a heterojunction with 2D materials, which could improve the performance of 2D photonic and optoelectronic devices.^{38–43} Ferroelectrics, as one of the smart materials, have a spontaneous electric polarization that occurs below the Curie temperature and reverses under an applied electric field. As reported previously, ferroelectric polarization can be modulated via incident light, while the light wavelengths can be tuned through switching the electric polarization.⁴⁴ Thereby, ferroelectrics can be utilized to improve the photonic and optoelectronic performances in 2D materials.

II. FUNDAMENTALS OF FERROELECTRICS

Ferroelectrics with robust spontaneous electric polarization have two or more discrete stable or metastable polarized states in zero applied electric field, and these polarized states can be switched

between each other under applied electric stimuli. Generally speaking, the concept of electric polarization is crucial to understand ferroelectricity. The electric polarization is associated with the separation between negative and positive charge centers along a specific direction of the crystal, which is defined as the electric dipole moment. The dipoles in the crystal can be reoriented to align by an applied electric field; therefore, the polarization direction can be changed under an external electric field.⁴⁵ The characteristics of the electric polarization in the ferroelectric response to an applied electric field are usually featured by hysteresis loops (P - E curves). As an effective and simple tool, the ferroelectric polarization measurement resulting in a P - E curve is the most common way to understand ferroelectrics, as illustrated in Fig. 2(a). The ferroelectricity of the crystal exists only in a certain temperature range. The spontaneous electric polarization disappears above a critical temperature, accompanied by the disappearance of the hysteresis loop. At this time, the crystal exhibits a structural transition from a polar ferroelectric phase to a non-polar paraelectric phase associated with a high symmetry structure, as shown in Figs. 2(b)–2(d). The phase transition might be first or second order, corresponding to polarization dropping to zero suddenly or gradually at phase transition temperature. This temperature is called the Curie temperature or Curie point.⁴⁵ It is important to note that all ferroelectric materials have their own Curie temperature.

Typically, ferroelectrics are insulators with asymmetry in the crystal structure. According to the symmetry in crystallography, ferroelectrics exist only in crystals with a unipolar axis. Of all 32 crystallographic point groups, only ten have special polar orientations, namely, 1, 2, m , $mm2$, 4, $4mm$, 3, $3m$, 6, and $6mm$.⁴⁶ For all ferroelectric crystals, their structures should belong to one of these ten point groups. The first discovery of ferroelectricity was reported in Rochelle salt in 1921 by Valasek. Several years later, a new system KH_2PO_4 (KDP) was discovered as a ferroelectric.⁴⁷ The modern

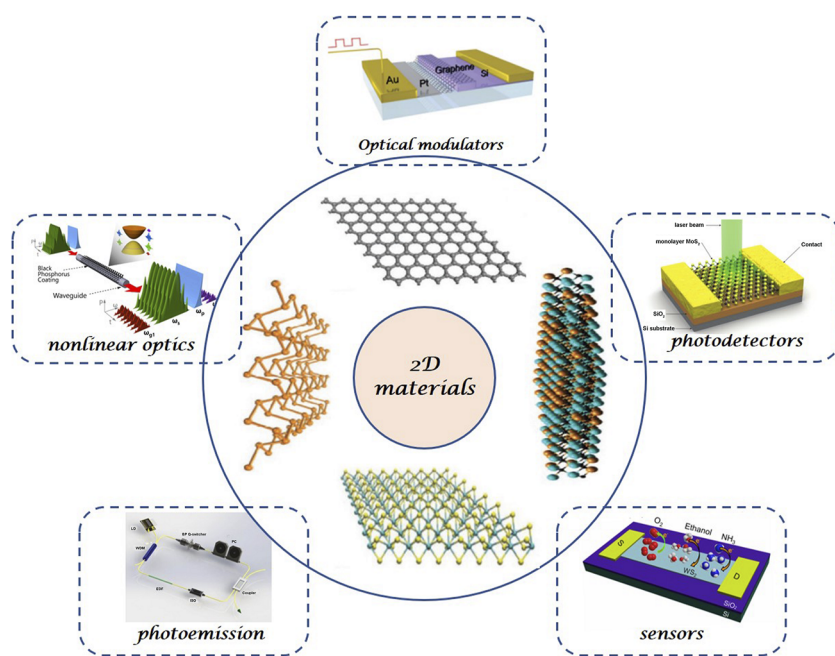


FIG. 1. 2D materials in photonics and optoelectronics.

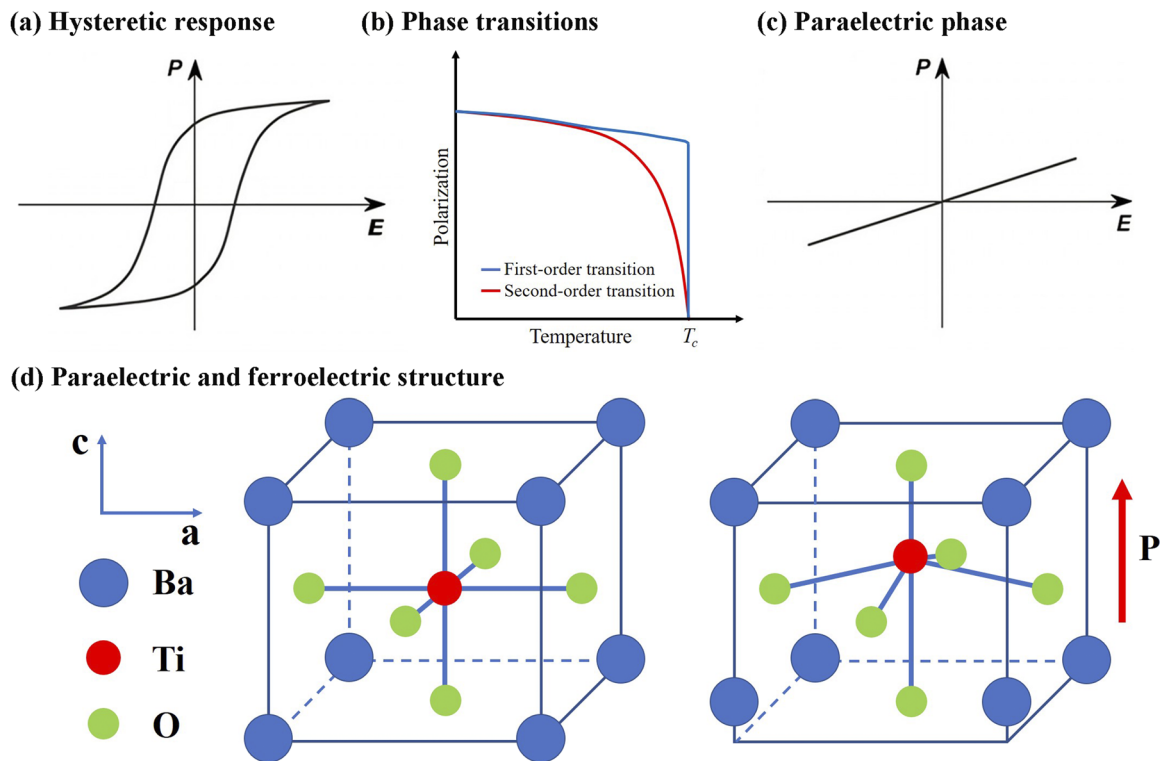


FIG. 2. Characteristics of ferroelectrics: (a) and (b) hysteretic response and phase transition of ferroelectrics, (c) electric polarization response curve of paraelectrics, and (d) corresponding crystal structures of paraelectric and ferroelectric phases.⁴⁵

era for ferroelectricity can be traced back to the Second World War, accompanied by the discovery of a simple perovskite BaTiO_3 (BT). So far, thousands of ferroelectrics have been discovered, and the typical ferroelectrics include inorganic perovskites (such as BaTiO_3), organic polymers (such as PVDF, polyvinylidene fluoride), perovskite molecular ferroelectric semiconductors (such as MAPbI_3), and 2D van der Waals materials (such as In_2Se_3).^{48–52}

As a subset of pyroelectrics and piezoelectrics,⁵³ ferroelectrics also exhibit other functional properties, such as piezoelectricity, dielectricity, pyroelectricity, and related effects (e.g., acoustic-optical effects, electro-optical effects, nonlinear optical effects, and photorefractive effects). The varieties of types and properties have made them particularly suitable for various applications.

III. MECHANISMS OF FERROELECTRICS ON 2D MATERIALS

Ferroelectrics have a spontaneous electric polarization, which can lead to dipole moments occurring in the direction perpendicular to the surface, resulting in net charges on the surface when the applied field is zero. The surface chemistry of ferroelectrics can be influenced in many ways as the bound charges are present on the surfaces. It can also be modulated by the external electric stimuli because of the ferroelectric polarization switching under an applied electric field. In addition, the electric charge could accumulate in ferroelectrics in response to applied mechanical stress and vice versa, which can lead to producing a local electric field or mechanical deformation. Thus, the interaction mechanisms of ferroelectrics

on 2D materials are mainly divided into three categories: interface charge effect, lattice strain effect, and carrier injection derived doping effect.

A. Interface charge effect

It is well known that field-effect transistors (FETs) have been widely used in numerous areas of the electronics industry. Most of the combinations of ferroelectric materials and 2D materials are based on the ferroelectric FET structure, which can be applied to sensors, memory devices, photodetectors, and pyroelectric detectors.^{54–58} For transistors based on 2D materials that act as channel semiconductors, ferroelectrics can be used instead of dielectric materials as gate dielectrics in FETs.^{59–62} Park *et al.*⁵⁹ reported a graphene monolayer on a h-BN FET-based ferroelectric PMN-PT $\{(1-x)[\text{Pb}(\text{Mg}_{1/3}\text{Nb}_{2/3})\text{O}_3]-x[\text{PbTiO}_3]\}$ substrate, as shown in Figs. 3(a) and 3(b). The ferroelectric polarization field could lead to charge-trapping at the interface between h-BN and PMN-PT, which can affect the charge transport in a 2D material. The bound charges that derived spontaneous polarizations of ferroelectrics could produce an ultrahigh electrostatic field at the interface between ferroelectrics and 2D materials, which can modulate the background carrier concentration with different polarized directions. As a result, it can give rise to total depletion/accumulation of carriers in the 2D material channel and depress the dark current,^{54,63} as shown in Figs. 3(c) and 3(d).

In addition, the ultrahigh ferroelectric field can modulate the band structure of 2D materials.^{54,64,65} Wijethunge *et al.*⁶⁴ constructed various configurations by encapsulating 2D materials using

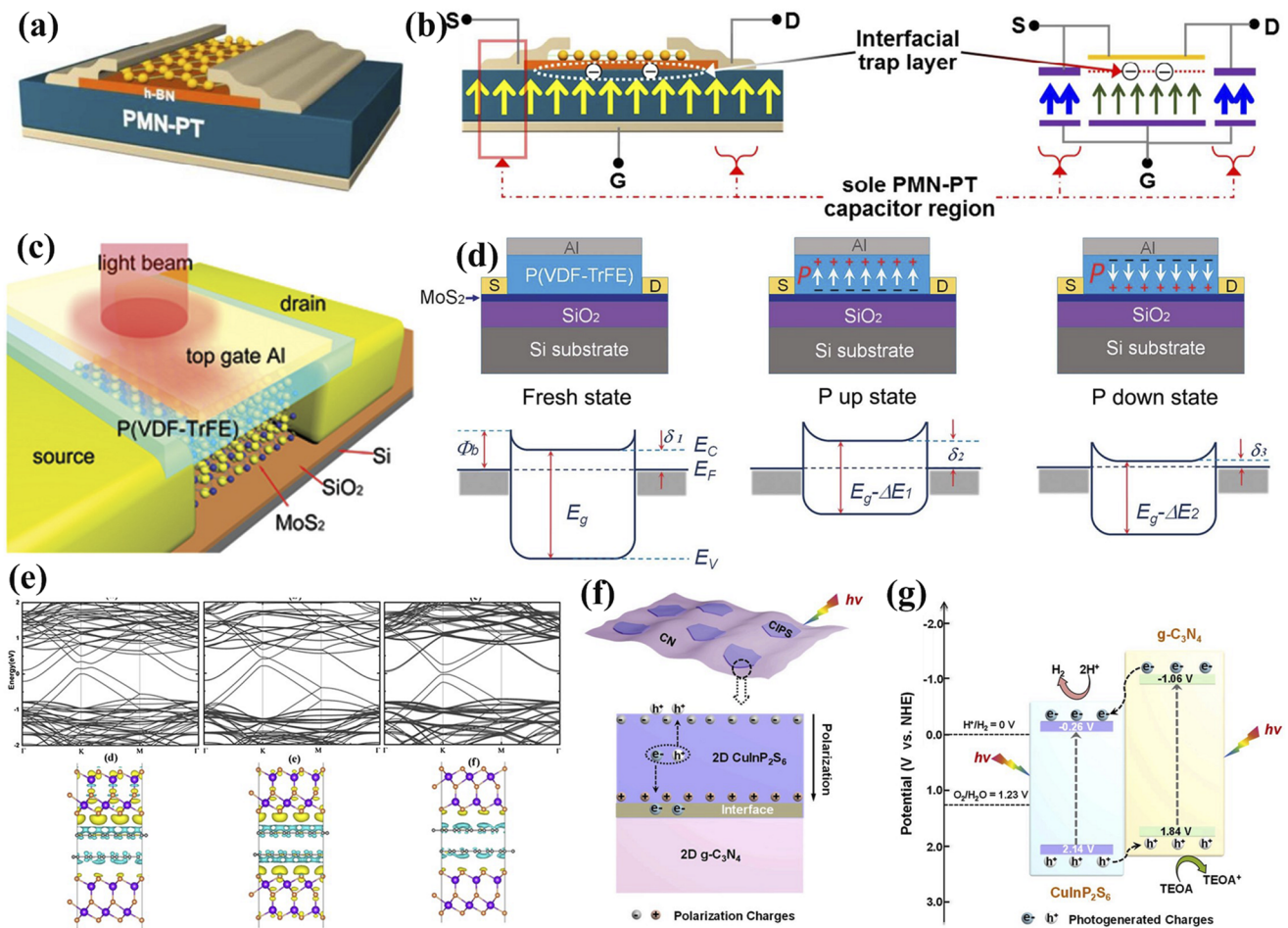


FIG. 3. Polarization derived interfacial charges on 2D materials: (a) schematic illustration of the ferroelectric FET; (b) cross-sectional view of the ferroelectric FET, including the interfacial trap layer;⁵⁹ (c) schematic illustration of the MoS₂ photodetector; (d) schematic diagram of the device and corresponding energy band in different polarization states;⁵⁴ (e) electronic band structure of various bilayer graphene/In₂Se₃ heterostructures and their corresponding charge density differences;⁶⁴ and (f) and (g) schematic illustration of the transfer of photogenerated charges.⁶⁷

2D ferroelectrics and investigated the band modulation in 2D material/ferroelectric heterostructures. As shown in Fig. 3(e), charge density arrangement and charge transfer at the contact surfaces should be changed by polarizing the ferroelectrics, which can lead to the modulation of the band structure. More interestingly, the electrostatic field could separate the photoexcited electrons and holes and prolong the carrier lifetime, thus improving the photogain of 2D material-based photodetectors or enhancing photocatalytic reaction with highly efficient charge transfer, as illustrated in Figs. 3(f) and 3(g).^{66,67} Therefore, the devices that use a local electric field generated by polarization to control the properties of 2D channel semiconductors can greatly improve performance and enrich the functions. Additionally, ferroelectrics also have excellent pyroelectric properties, that is, a change in temperature makes their electrical polarization cause a difference across the material and the interface charge distribution changes; thereby, infrared light can be used to control the resistance of 2D

devices. Under infrared light, the thermoelectric response of ferroelectrics can transform into the resistivity modulation of the 2D devices; thereby, it perhaps achieves room temperature infrared detection.⁶⁸

B. Lattice strain effect

The photonic and optoelectronic properties of semiconductors can be significantly improved through tuning their band structures. As mentioned above, the band structure can be modulated by using ferroelectric-based 2D material/ferroelectric heterostructures owing to different responses to each contact surface. In addition, strain engineering is an effective strategy for tuning the electronic structure and lattice of 2D materials and thus modulating the bandgap.^{69–72} Therefore, combining 2D semiconductors with ferroelectrics, the energy bandwidth can also be tuned by strain engineering due to inverse piezoelectricity for adjusting the crystal structure of the

2D materials.^{42,73–77} As shown in Figs. 4(a) and 4(b), Hui *et al.* developed an electromechanical device whose biaxial compressive strain can be applied via a piezoelectric substrate to MoS₂.⁴² When an external electric field is applied to ferroelectrics PMN-PT, the electric dipoles gradually tend to orient along the direction of the applied electric field and cause the crystal to shrink or expand in a certain direction. The in-plane strain of the ferroelectrics can be transmitted to MoS₂ of the adjacent layer through the interface, thereby generating the lattice strain to tune the band structure. The effect of tunable strain is also suitable for other 2D materials, such as graphene [Figs. 4(c)–4(e)].⁷⁴ The piezoelectric field-induced strain engineering in the 2D materials opens an avenue to enhance the performance of 2D optoelectronics. Compared to chemical doping and defect engineering, the strain engineering provides a non-destructive approach to modulate the band structure of 2D materials.

C. Doping effect

The P–n junction is crucial for the preparation of 2D semiconductor nanodevices with advanced functionalities, and the control of its carrier type and concentration is needed. How to achieve controllable doping of 2D semiconductor materials has become an obstacle to the functionalization of devices. The current research methods are generally insufficient. However, the remanent polarization of ferroelectrics can be used to electrostatically dope 2D

semiconductors. Controlling the polarization direction of ferroelectrics, the carrier injection can be modulated to realize p-type and n-type doping.^{37,39,55,78} For example, Lv *et al.*³⁹ reported local patterned ferroelectric polarization that resulted in p–n doping in MoS₂ optoelectronic devices as shown in Figs. 5(a) and 5(b). The ferroelectrics P(VDF-TrFE) are in contact with MoS₂, which achieve the carrier doping in MoS₂ by local polarization. An AFM tip is employed on ferroelectrics to switch the local polarization to engineer the p- and n-type doping in MoS₂. Guan *et al.*³⁷ prepared graphene-based LiNbO₃ photodetectors, as shown in Fig. 5(c). As the pyroelectric effect of ferroelectrics, laser irradiation can generate local ferroelectric polarization on LiNbO₃, which produces a thermal current. However, it may generate a reverse current without light [Fig. 5(d)]. The types of charges accumulated on both sides of electrodes 1–3 and electrodes 2–4 are opposite, while the charges accumulated by electrodes 1–2 and electrodes 3–4 are the same. The accumulated charges doped at the graphene surface resulted in a p–n type graphene homojunction. As illustrated in Fig. 5(e), p-type doping was performed at electrodes 1–3 and n-type doping at electrodes 2–4 on light.

IV. PHOTONICS AND OPTOELECTRONICS OF FERROELECTRICS/2D MATERIALS

Since their discovery, 2D materials have been widely used in photonics and optoelectronics. Until now, a mass of 2D materials

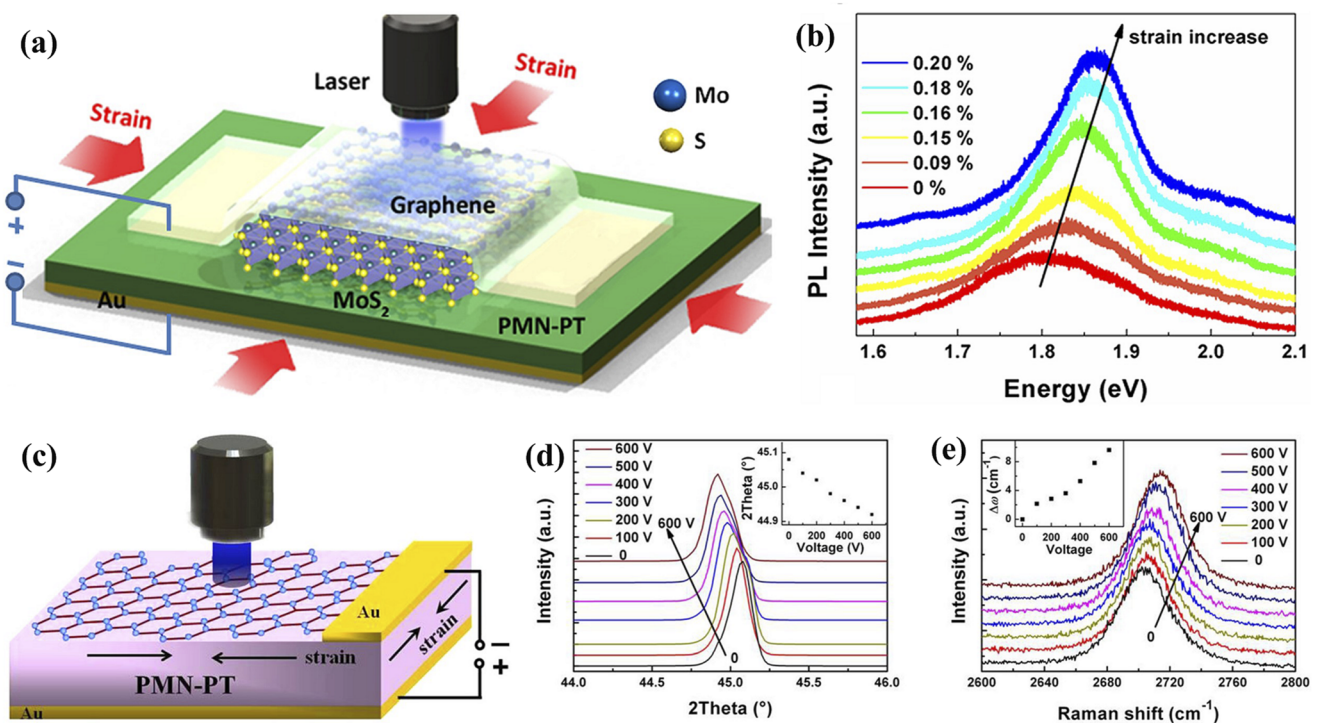


FIG. 4. Tunable strain of ferroelectrics on 2D materials: (a) schematic diagram of the PMN-PT/MoS₂ hybrid system, (b) PL spectra of MoS₂ under various strains,⁴² (c) schematic diagram of the PMN-PT/graphene heterostructure, (d) PMN-PT (002) peaks of XRD with different bias voltages, and (e) 2D peaks of graphene at different bias voltages.⁷⁴

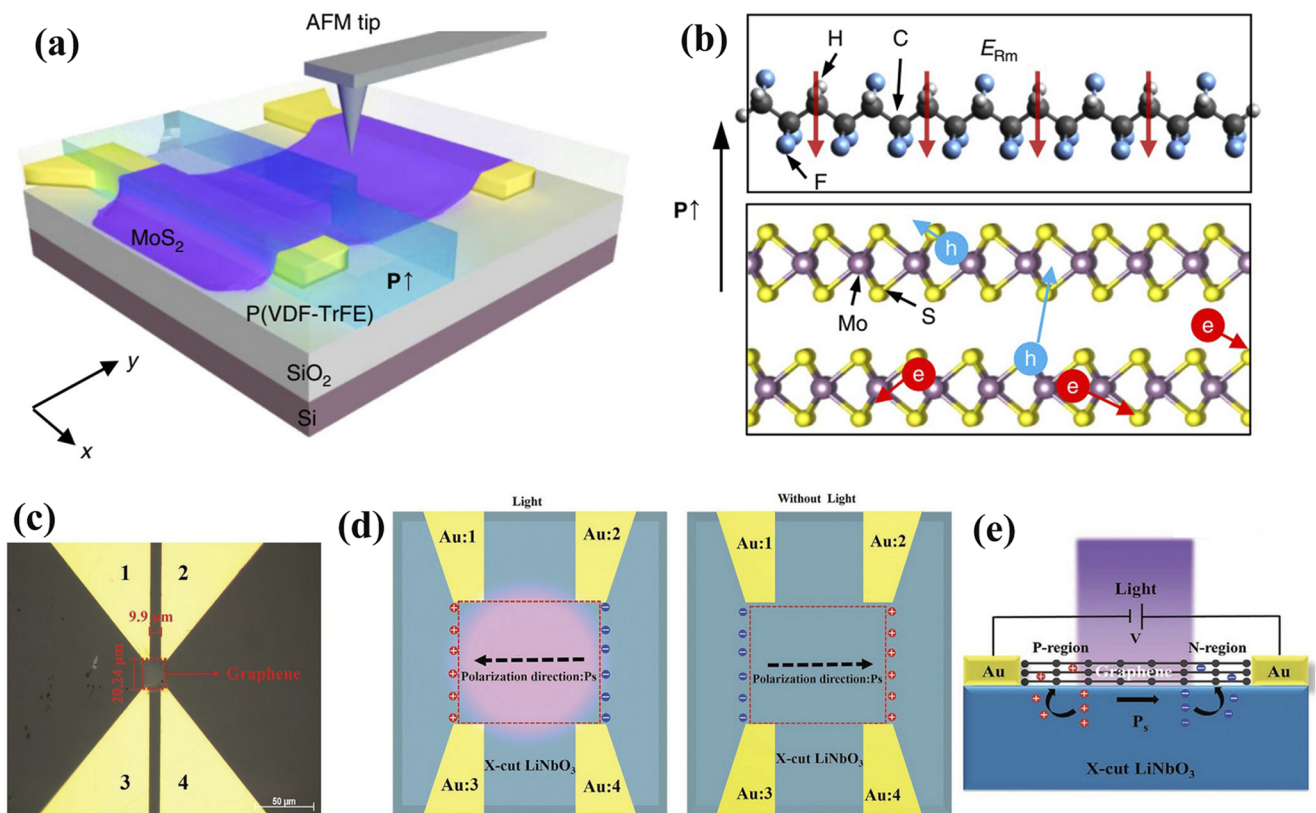


FIG. 5. Ferroelectric polarization caused doping of 2D materials: (a) schematic diagram of a ferroelectric-coupled MoS₂ device using an AFM tip as the poling electrode; (b) coupling between upward polarization in ferroelectrics and carriers in MoS₂, which can lead to accumulated holes near the interface;³⁹ (c) optical microscopy image of the graphene-based LiNbO₃ photodetector; (d) charge distribution when the device is illuminated or not illuminated; and (e) photodetector at the p–n junction state.³⁷

have been prepared and numerous unique optical and electronic performances have been discovered. To be associated with layers bound by weak van der Waals forces, the photonic and optoelectronic performances of 2D materials should be optimized by changing the number of layers, thicknesses, and intercalation to tune the band structure. In addition to these, combining 2D materials with various other functional materials (such as dielectrics, semiconductors, metals, and organic materials) can also expand the fundamental and applied research of 2D materials. Among these functional materials, ferroelectrics have been extensively studied because of their spontaneous electric polarization and strong inverse piezoelectric effects, as well as the characteristics of the large dielectric coefficient. Combining 2D materials with ferroelectrics can take into account the advantages of both to improve the optical properties of devices. By applying electric fields to 2D material/ferroelectric heterostructures, one can achieve the modulation of the photonic and optoelectronic performances in 2D materials. For the past few years, an increasing number of hybrid systems combining 2D materials with ferroelectrics have been used to produce high-performance photonic and optoelectronic devices.^{37,44,54,62,79–83}

A. Graphene/ferroelectric hybrid system

As the first member of the 2D family, graphene is widely used in the research of FETs. Traditional FETs mainly use insulating materials, such as SiO₂, as gate dielectrics. Graphene has been reported to have electron mobilities ranging from 10^3 to 10^4 cm² V⁻¹ s⁻¹ in the form of graphene/SiO₂ FETs.⁸⁴ Ferroelectric FETs fabricated by using ferroelectrics as gate dielectrics instead of the insulating dielectric layer SiO₂ can effectively improve the mobility of graphene.^{38,85,86} Guo *et al.* proposed a tunable long wave infrared photodetector based on the graphene/ferroelectric heterostructure. They found that the periodically polarized ferroelectric domains can apply a local electrical field at the interface of the ferroelectric layer and graphene, which enables the graphene plasmonic photodetector have the characteristics of an ultra-high responsivity of 7.62×10^6 A W⁻¹ and a detectivity of 6.24×10^{13} Jones over a broad infrared detection range of 5–20 μm at room temperature,⁸⁷ as illustrated in Figs. 6(a)–6(d). The nanoscale ferroelectric domains can facilitate the spatial regulation of carrier density in graphene, which can tune the optical and electronic properties of graphene and consequently enhance its absorption of incident photons.⁸⁸

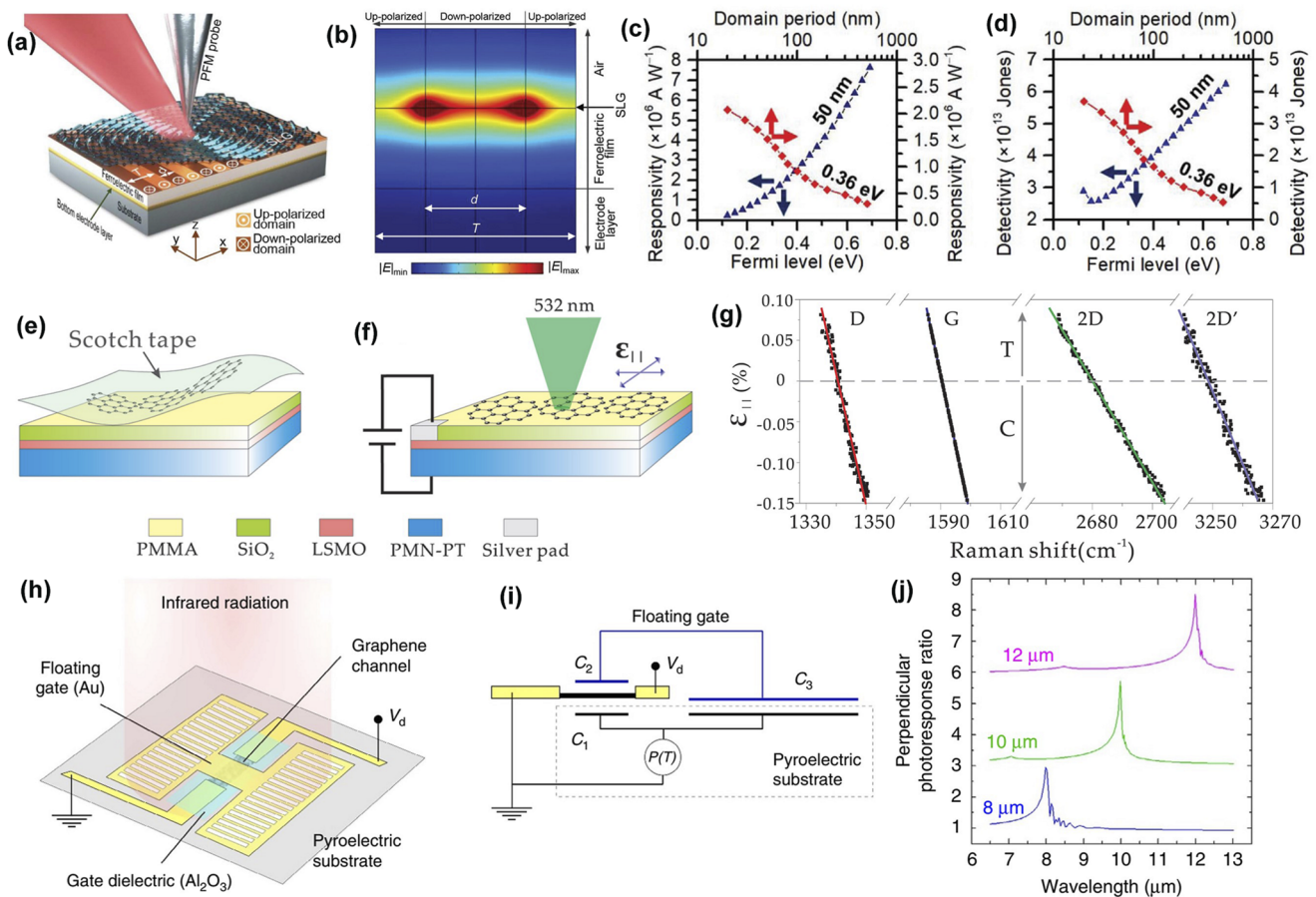


FIG. 6. Graphene/ferroelectric hybrid systems: (a) diagram of the graphene photodetector, (b) ferroelectric domains control the electric field distribution in (a), (c) photoresponsivity and (d) detectivity of the device,⁸⁷ (e) exfoliated graphene transferred onto the PMN-PT substrate, (f) diagram of in-plane biaxial strain applied to graphene, (g) Raman features of graphene related to the biaxial strain,⁷³ (h) schematic diagram of the pyroelectric bolometer based on graphene, (i) working mechanism diagram in (h), and (j) simulated total absorption for the devices.⁶⁸

The PMN-PT single crystal, as one of the ferroelectrics with excellent piezoelectric properties, is widely used in optical devices because of its electric and optical properties. As shown in Figs. 6(e)–6(g), Ding *et al.*⁷³ used the PMN-PT single crystal as a piezoelectric actuator to provide tunable biaxial stresses (both tensile and compressive) to single-layer graphene. The strain is transferred to graphene through the interface, causing the Raman peak position of graphene to shift linearly with both the tensile strain and compressive strain, which can be used to tune the band structures and electronic properties of graphene. Combining graphene with the piezoelectric has been promised as an important route to tailor the optoelectronic and electronic properties of graphene.

Pyroelectricity, having temperature-sensitive polarization, is also an important characteristic of ferroelectrics. For instance, Sassi *et al.*⁶⁸ demonstrated a mid-infrared photodetector based on single-layer graphene (SLG) on the LiNbO₃ crystal substrate

by depositing a floating gate, as shown in Figs. 6(h)–6(j). Under IR radiation, LiNbO₃ can generate a pyroelectric charge ΔQ on capacitor C₃, eventually leading to the modulation of SLG channel conductivity. As a result, a responsivity of $\sim 0.27 \text{ mA W}^{-1}$ and a large temperature coefficient of resistance (TCR) of $\sim 900\%/K$ are obtained. Additionally, as mentioned previously, Guan *et al.*³⁷ found that local ferroelectric polarization can be achieved using laser irradiation on LiNbO₃ due to the pyroelectric effect, leading to graphene being doped by the positive or negative charges. The formation of the p–n junction through doping graphene can improve the light-detection capability of devices, showing a wide detection range from 405 to 2000 nm and a high responsivity of $\sim 2.92 \times 10^6 \text{ A W}^{-1}$, as well as a high detectivity of $\sim 8.65 \times 10^{14}$ Jones. Thus, combining graphene with ferroelectrics might enable future explorations and apply for photonic and optoelectronic applications, such as non-volatile memories, photodetectors, and phototransistors.^{89–95}

B. Transition metal dichalcogenide/ferroelectric hybrid system

Transition metal dichalcogenides (TMDs), as a member of 2D materials, have a structure similar to that of graphene but with a non-zero bandgap. TMDs are the compounds of type MX_2 ($M = \text{W}, \text{Mo}, \text{Pt}, \text{and Pd}; X = \text{S}, \text{Se}, \text{and Te}$). Numerous research studies show that TMDs are strain-tunable;^{6,71} thereby, TMDs, in particular, are more favored for strain engineering, which can tune their electronic, photonic, and spintronic properties. The strain generated by the lattice mismatch between TMDs and the ferroelectric substrate can tune the electronic structure and phonon spectrum.⁴²

The ferroelectric field effect is also a basic research method for tuning and improving the performance of TMDs. The essence of the ferroelectric field to modulate the photoemission of 2D materials is to modulate the channel carriers. Many researchers have combined the ferroelectrics with MoS_2 to fabricate FET photoelectronic devices. In these 2D devices, ferroelectrics are usually used as

the gate dielectrics.^{80,81,96,97} As illustrated in Fig. 7(a), Chen *et al.*⁹⁶ designed a new type of FET using 2D MoS_2 and P(VDF-TrFE). The ferroelectric material P(VDF-TrFE) acts as the gate dielectric, while MoS_2 acts as the channel. The polarization of P(VDF-TrFE) can produce an ultrahigh local electrostatic field on the MoS_2 surface, which is much larger than that generated by an external gate voltage in other traditional FETs. Thus, it can facilitate the enhanced carrier mobility of MoS_2 , which can achieve a broad range photoresponse from visible to $1.55 \mu\text{m}$ and result in a high sensitivity of 346.24 A/W under 20 nW illumination of 450 nm [Figs. 7(b) and 7(c)]. In addition to MoS_2 , other TMD materials have also been used to prepare ferroelectric FET devices with further investigation.^{98–103} As a result, high performance can be achieved, such as fast and stable photoresponse, low dark current, and broad spectral range detection under light ranging from visible to near infrared.

Negative capacitance behavior in ferroelectrics has so far been promised to reduce the energy dissipation of electronics.

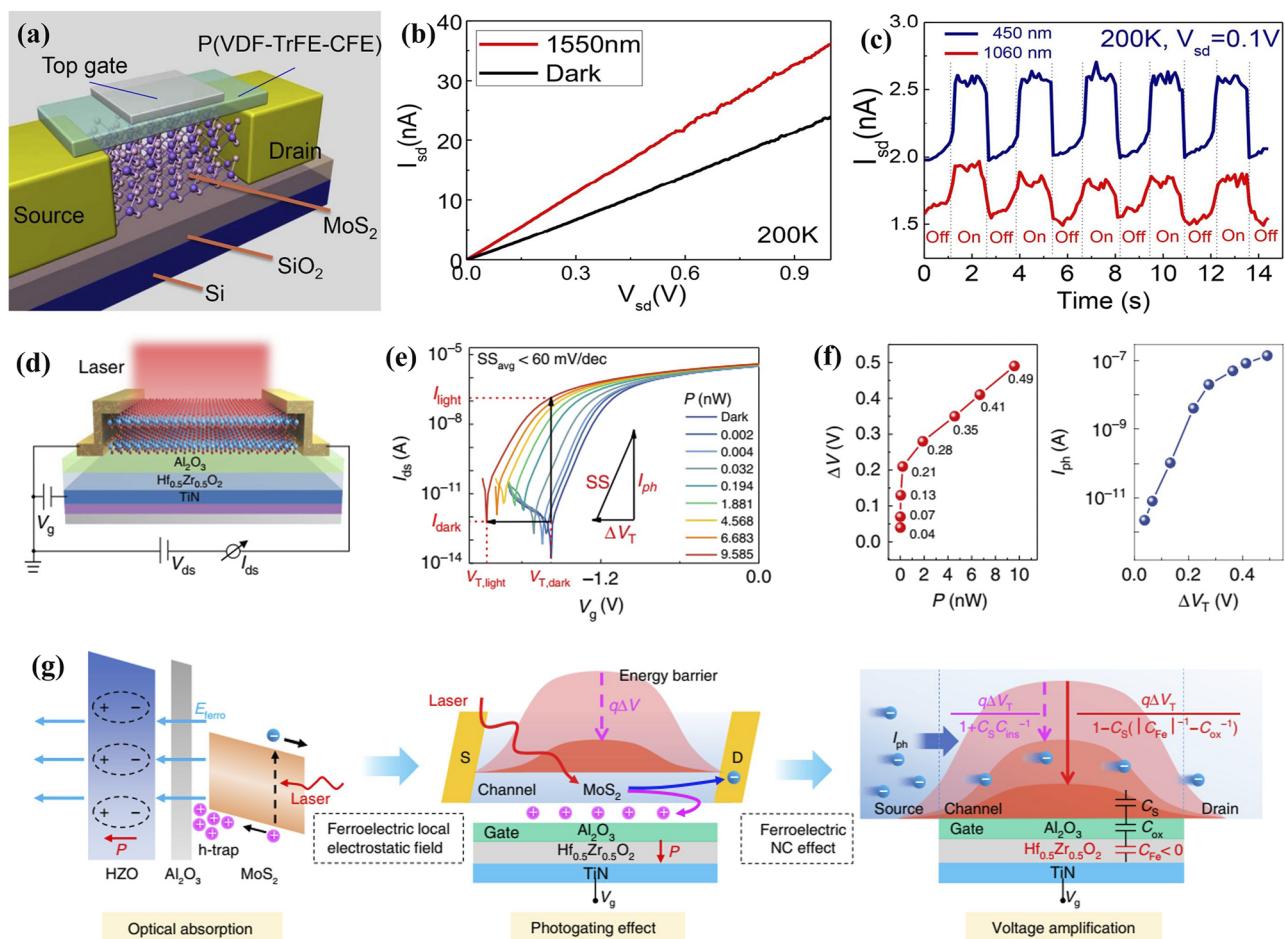


FIG. 7. TMD/ferroelectric hybrid systems: (a) schematic view of MoS_2 ferroelectric FETs, (b) and (c) optical properties of MoS_2 ferroelectric FETs,⁹⁶ (d) schematic diagram of negative capacitance MoS_2 phototransistors, (e) V_g – I_{ds} curves at $V_{ds} = 0.5 \text{ V}$ in the dark and at various incident light powers, (f) dependence of threshold shifts on the incident optical powers and photocurrent vs threshold shifts extracted from (e), and (g) mechanism of optical detection in the negative capacitance MoS_2 phototransistors.⁶³

The voltage across the rest of the circuit can be enhanced by a local negative capacitance. Negative capacitance FETs, as a new type of structure, are expected to break through the Boltzmann limit and address the power consumption requirements for increasingly dense integrated circuits.^{63,104–106} On the other hand, the electrostatic local field derived from ferroelectrics can separate the photoexcited electron–hole pairs, resulting in a strong photogating effect on 2D optoelectronic devices, which forces more electrons to cross the energy barrier and forms photocurrent. Tu *et al.*⁶³ proposed and fabricated negative capacitance 2D MoS₂ phototransistors using a ferroelectric Hf_{0.5}Zr_{0.5}O₂ film in the gate dielectric stack, as shown in Fig. 7(d). Under the influence of the ferroelectric NC effect and ferroelectric electrostatic local field, the MoS₂ photodetectors exhibited an ultra-steep sub-threshold slope of 17.64 mV/dec and an ultrahigh photodetectivity of 4.75×10^{14} cm Hz^{1/2} W⁻¹ at room temperature with lower dark current [Figs. 7(e)–7(g)].

So far, electrostatic doping by a non-volatile remanent polarization electric field of ferroelectrics is considered as a potential solution to 2D TMD doping.^{39,55,56,79,101} As demonstrated in Fig. 8(a),⁵⁶ both p- and n-type MoTe₂ can be obtained via carrier injection and form a lateral homojunction. The polarization state of the ferroelectrics can modulate the carrier type. In detail, the polarization direction of ferroelectric copolymers P(VDF-TrFE) deposited on MoTe₂ was controlled using scanning probes, and then, the p-type doping in MoTe₂ was achieved by the accumulation of holes or depletion of electrons in MoTe₂, while the n-type doping occurs in the opposite direction. As a photodetector, the p–n homojunction devices possess efficient self-powered detection and good optoelectronic properties, such as high photoresponsivity, high external quantum efficiency, fast response time, and high specific detectivity [Fig. 8(b)]. Using this method, in the TMD/ferroelectric

hybrid system, lateral n–p, p–n, p–p, and n–n homojunctions can be arbitrarily formed and altered via controlling the polarization state of the ferroelectrics.

In addition to electrostatic doping, the non-volatile remanent polarization electric field of ferroelectrics also leads to the non-volatile multilevel memory effect, which can be used as synaptic weight elements of neural network hardware.^{107–109} As shown in Fig. 8(c), Luo *et al.*¹⁰³ investigated a hybrid optoelectronic 2D memristive transistor consisting of a piezoelectric transducer (PbZr_{0.2}Ti_{0.8}O₃) as the gate dielectric and WS₂ as the conducting channel. The non-volatile ferroelectric polarization of PZT can modulate the transport properties of WS₂, while the light absorption of WS₂ can switch the ferroelectric polarization of PZT. The conduction states in the WS₂ channel can be controlled by light and voltage through the ferroelectric field effect. A short-term potentiation to long-term potentiation transition induced by light occurs through the enhanced memory retention with increasing light intensity [Fig. 8(d)]. This is very similar to the memory retention of biological memory systems. Thus, leveraging on the light-induced long-term and short-term synaptic behaviors in hybrid optoelectronic 2D memristive transistors, they can be used for neuromorphic visual synaptic devices and to realize brain-like learning and memory.

C. Other 2D semiconductor/ferroelectric hybrid system

Black phosphorus (BP), another direct bandgap semiconductor with a bandgap from 0.3 eV to greater than 2 eV, exhibits good photoelectric properties over a wide spectral range from mid-infrared to visible wavelengths. Constructing ferroelectric heterostructures by combining BP with ferroelectrics is usually expected to build ferroelectric field-effect transistors. In general, the BP ferroelectric

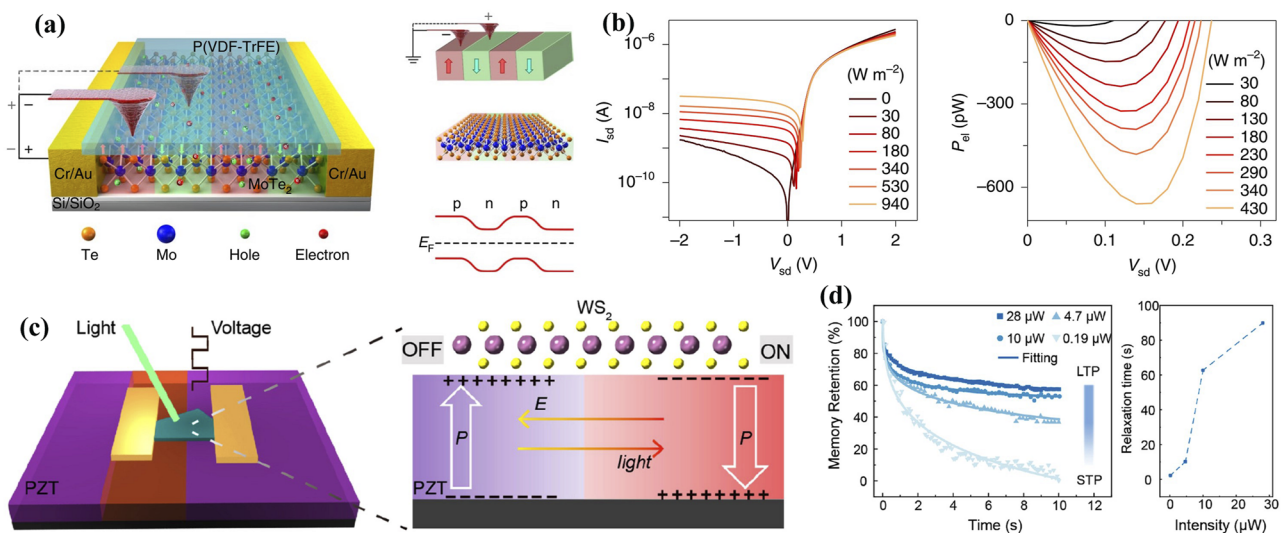


FIG. 8. (a) Schematic of doping in MoTe₂ using a PFM controlled polarization direction of P(VDF-TrFE). (b) Photoresponse of the p–n homojunction.⁵⁵ (c) Schematic diagram of 2D memristive transistors and mechanism of electrically and optically tunable WS₂ channel conductance. (d) Memory retention and relaxation time depend on the intensity of light.¹⁰³

FETs exhibited high linear mobility values and high on/off ID ratios, which will be appropriate for nonvolatile memory devices.^{110–113} As shown in Figs. 9(a) and 9(b), Xie *et al.* designed and developed a non-volatile photoelectric memory device with “electrical writing–optical reading” mode based on BP/PZT heterostructure ferroelectric FETs. By controlling the polarization state of PZT, the ferroelectric FET device exhibits different photoresponse modes of positive and negative photoconductivities at various polarization states. On the basis of the polarization-dependent photoresponse, the net photocurrent can be used as the readout signal in the device, and the optical reading in this device can be extremely stable compared to the electrical reading in conventional FET memory devices. Based on this, the photoelectric-type ferroelectric FET memory device can exhibit reliable data retention and fatigue performance with very low energy consumption.

The emerging bismuth layered oxyseelenide ($\text{Bi}_2\text{O}_2\text{Se}$), benefiting from high electron mobility and being ultrafast and highly sensitive in a broad optical spectrum, has great potential for optoelectronic and electronic applications. As shown in Fig. 9(c),

Yan *et al.*¹¹⁴ constructed 2D ferroelectric FETs with epitaxial growth of the $\text{Bi}_2\text{O}_2\text{Se}$ film on PMN-PT substrates. The polarization state of PMN-PT in ferroelectric FETs can modulate the carrier density of the $\text{Bi}_2\text{O}_2\text{Se}$ film [Fig. 9(d)] and facilitate it to have a response to external stimuli (including optical and electrical). Specifically, the device exhibits a polarization-dependent photoresponse under visible light and infrared light illumination [Figs. 9(e) and 9(f)], demonstrating the application of devices for optoelectronic coincidence detection. Thus, the reversible and nonvolatile manipulation of the carrier density of 2D materials can be achieved through switching the ferroelectric polarization at room temperature.

D. 2D semiconductor/2D ferroelectric hybrid system

In recent years, the van der Waals ferroelectrics have emerged as a new class of ferroelectric materials.^{115–121} It is interesting to combine 2D semiconductors with 2D ferroelectrics to form 2D heterostructures in one vertical stack. Held together by van der Waals forces as free from dangling bonds, such heterostructures allow a far

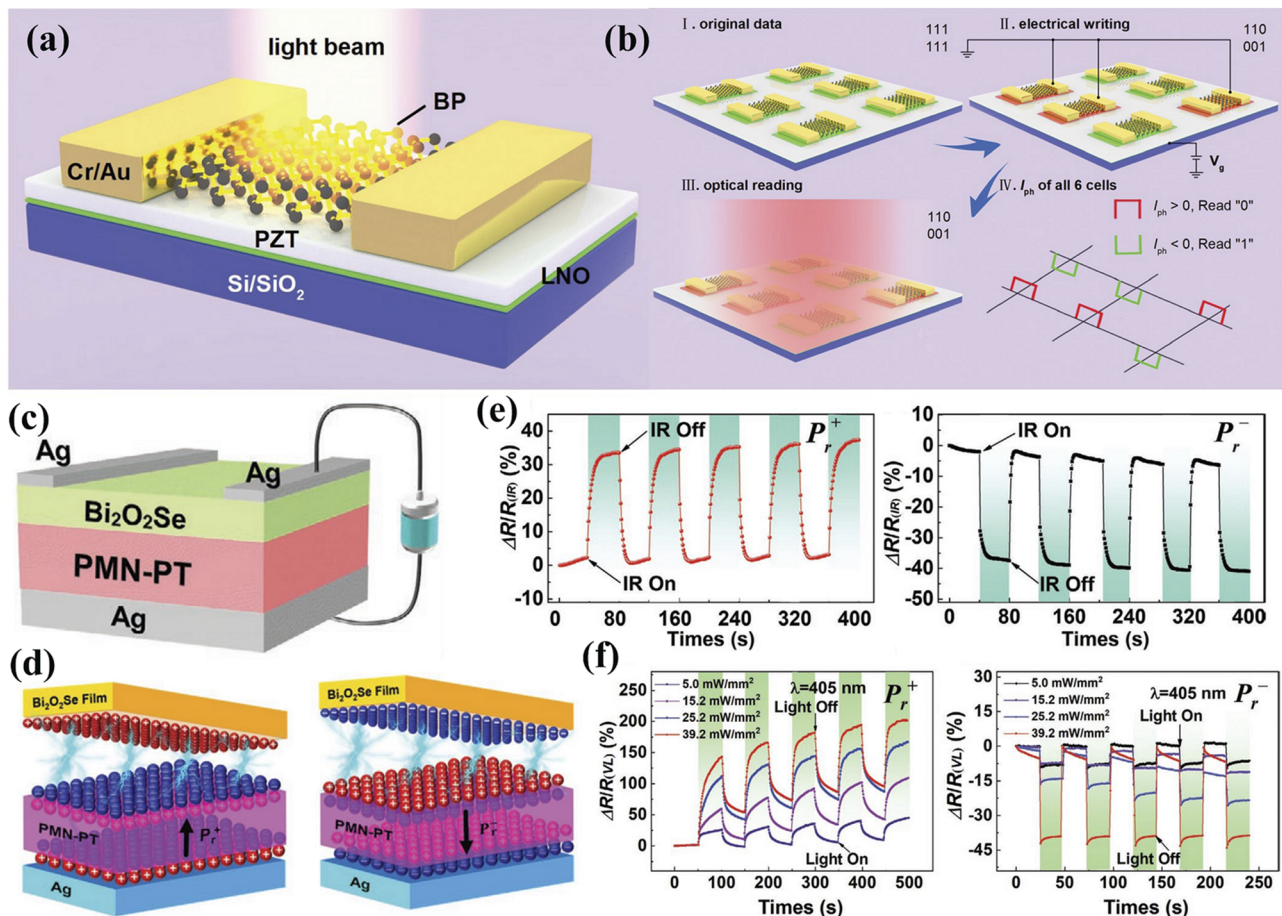


FIG. 9. (a) Schematic diagram of BP/PZT heterostructure ferroelectric FETs. (b) Schematic illustration of a 6-cell photoelectric memory device.¹¹³ (c) Schematic diagram of the $\text{Bi}_2\text{O}_2\text{Se}$ /PMN-PT ferroelectric FET structure. (d) Schematic view of the manipulation of the electron carrier density of the $\text{Bi}_2\text{O}_2\text{Se}$ film via polarization switching. (e) and (f) Electronic properties of IR and visible light illumination on $\text{Bi}_2\text{O}_2\text{Se}$ films.¹¹⁴

greater number of combinations than traditional 3D semiconductor heterostructures.^{122,123} The unique 2D heterojunction interface, as well as the spontaneous polarization of ferroelectrics, enables exotic interface interaction and carrier dynamics, which can lead to the realization of high-performance photonics and optoelectronics, such as ultra-low-power consumption ferroelectric FETs, excellent optoelectronic synaptic behaviors for memory and logic operations, and broadband ultrafast photodetection.^{65,124–131}

As typical representatives of 2D van der Waals ferroelectrics, both In_2Se_3 and CuInP_2S_6 demonstrate stable room temperature ferroelectric performance, which are important for practical

applications based on ferroelectrics. As shown in Fig. 10(a), Li *et al.*¹³¹ studied the electrostatic coupling phenomena of vdW $\text{MoS}_2/\text{CuInP}_2\text{S}_6$ heterostructures. A lot of negative charges were injected from the tip and trapped at the $\text{MoS}_2/\text{CuInP}_2\text{S}_6$ interface when polarization reversed to the upward state, whereas the positive charges were injected with downward polarization. Charge injection during the polarization switching seems the governing field effect, which can tune the photoluminescence and electronic performances of MoS_2 . On the other hand, the polarization performance of CuInP_2S_6 would be influenced by the photoactivity of MoS_2 . For 2D ferroelectric In_2Se_3 , Guo *et al.*¹³⁰ proposed an optoelectronic

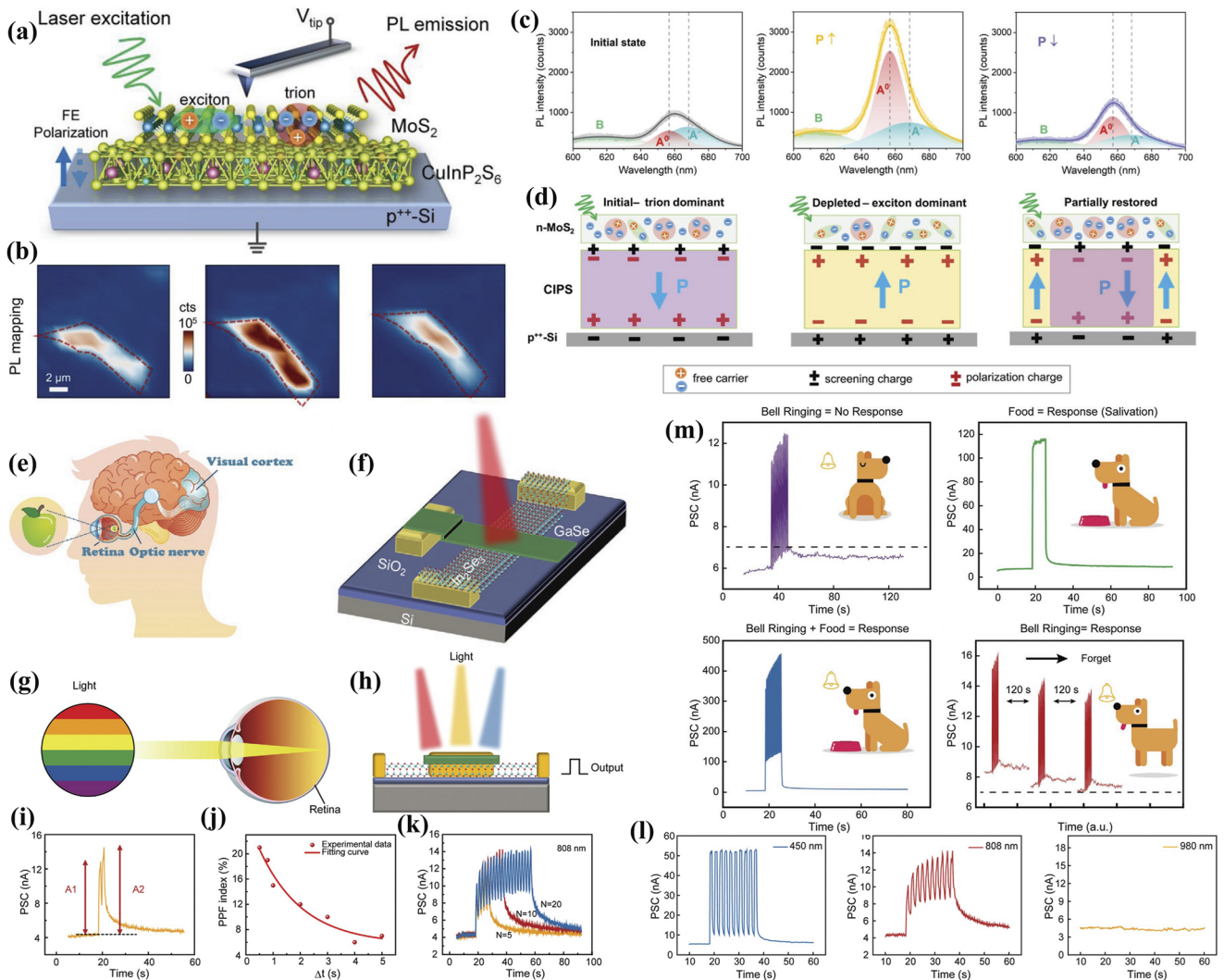


FIG. 10. 2D semiconductor/2D ferroelectric hybrid systems: (a) schematic diagram of the $\text{MoS}_2/\text{CuInP}_2\text{S}_6$ heterostructure, (b) photoluminescence mapping images of the $\text{MoS}_2/\text{CuInP}_2\text{S}_6$ heterostructure in the initial state after -6 and $+8$ V switching, (c) photoluminescence spectra of different polarization states, (d) corresponding microscopic model of exciton and trion emissions for (b) and (c),¹³¹ (e) schematic illustration of the biological visual system, (f) structure of the optoelectronic synaptic device, (g) working mechanism of the retina, (h) schematic diagram of the optoelectronic synaptic device under light stimuli to mimic the retina, (i) postsynaptic current triggered by a pair of light pulses, (j) paired-pulse facilitation index vs light pulse interval time Δt , (k) postsynaptic current triggered by several consecutive light pulses, (l) responses of postsynaptic current under 10 light pulses with different wavelengths, and (m) Pavlov's dog experiments under electrical and light stimuli.¹³⁰

synaptic device based on the 2D van der Waals heterojunction composed of 2D ferroelectric In_2Se_3 and 2D semiconductor GaSe and used it to mimic the biological visual system. The reversible spontaneous polarization of In_2Se_3 can be used to tune the conductance of optoelectronic synaptic devices, thus realizing the simulation of synaptic dynamics. The optoelectronic synaptic devices can not only convert light stimuli into electrical signals but also recognize colors like the retina as with the case of the wavelength selectivity. This response characteristic of optoelectronic synaptic device is similar to that of the retina under light stimuli. In addition, Pavlov's dog experiment was conducted using light pulses defined as food to cause salivation and electrical pulses defined as bell to trigger a conditioned response, which demonstrated the ability of the device to treat complex optical and electrical inputs.

V. OPPORTUNITIES AND OUTLOOK

In this Perspective, we showed the photonic and optoelectronic properties of the hybrid systems combining 2D materials with ferroelectrics. For example, in graphene-ferroelectric heterostructures or graphene-based ferroelectric FETs, ferroelectric polarization can apply a local electrostatic field to graphene to enhance carrier mobility and the absorption of incident photons, resulting in ultra-high photoresponsivity and detectivity. Additionally, controlling the two polarized directions of ferroelectrics, the carrier concentration can be effectively modulated to realize p-type and n-type doping in graphene to form a p-n junction, leading to a wide detection, high responsivity, and detectivity. Moreover, since the remnant polarization exists at zero electric field, the graphene/ferroelectric device has lower energy dissipation. As graphene is also a stress-tunable material, the band structure and electronic properties of graphene can be modified by the provided stresses from ferroelectrics due to the inverse piezoelectric effect in graphene/ferroelectric systems, which can achieve the improvement of graphene performance. The modulation of graphene combining it with ferroelectrics is also applicable to TMDs and other 2D materials. For ferroelectric TETs based on MoS_2 , ferroelectrics instead of traditional dielectrics act as the gate dielectrics and MoS_2 as the channel. The ferroelectric polarization produces an ultrahigh local electrostatic field on the MoS_2 surface, which can facilitate the enhanced carrier mobility of MoS_2 and achieve a broad range photoresponse and a high sensitivity. Meanwhile, the local electrostatic field can separate the photoexcited electron-hole pairs, resulting in a strong photogating effect on MoS_2 -based optoelectronic devices, which forces more electrons to cross the energy barrier and forms photocurrent, achieving ultrahigh photodetectivity at room temperature with lower dark current. Ferroelectrics have rich physical properties, such as ferroelectricity, piezoelectricity, dielectricity, and pyroelectricity, which may be used to modulate 2D materials with a variety of functions. Although more and more 2D material/ferroelectric systems have been investigated and the performances of 2D materials have been significantly improved in recent years, the research of ferroelectrics on 2D materials is still in its infancy, and there are still many problems to be solved to realize 2D nanodevice applications based on 2D material/ferroelectric hybrid systems.

The process of preparing 2D material/ferroelectric nanodevices often involves the large-scale transfer of 2D materials. How

to not damage the 2D materials or reduce their performance during the transfer process requires further exploration. There are many influencing factors at the 2D material/ferroelectric interfaces (charge, strain, interface, surface trap states, etc.). What might happen if coupling 2D materials to ferroelectrics with various properties. Despite recent activity, the intrinsic mechanism of the 2D material/ferroelectric interfaces and modulation of 2D materials by ferroelectric polarization are not completely investigated and understood. In addition, the repeatability and stability of 2D nanodevices based on the 2D material/ferroelectric hybrid system need to be improved. Moreover, new 2D materials/ferroelectric devices need to be discovered and explored. Furthermore, considering this enormous number of combinations, theoretical guidance is needed in future research. The above issues and challenges are of great interest from basic research to industrial applications. The developments of prototype nanodevices combining 2D materials with ferroelectrics and the improvement in performances of 2D materials have potential to drive future innovation in the photonic and photoelectronic industry. Combining 2D semiconductors with ferroelectrics, electrostatic doping in 2D semiconductors by a non-volatile remanent polarization electric field of ferroelectrics is considered as a potential solution to 2D semiconductor doping.

ACKNOWLEDGMENTS

We acknowledge financial support from the National Natural Science Foundation of China (Grant No. 61905157), the Natural Science Foundation of Hunan Province, China (Grant No. 2021JJ40446), the Key Project of Department of Education of Guangdong Province (Grant No. 2018KCXTD026), and the Science and Technology Innovation Commission of Shenzhen (Grant Nos. JCYJ20170818093453105 and GJHZ20180928160209731). This project was supported by the State Key Laboratory of Luminescence and Applications (Grant No. SKLA-2020-03) and also funded by the Deanship of Scientific Research (DSR), King Abdulaziz University, Jeddah (Grant No. KEP-MSc-70-130-42). The authors acknowledge the DSR for technical and financial support. The Deanship of Scientific Research (DSR) at King Abdulaziz University, Jeddah, Saudi Arabia has funded this project, under Grant No. FP-159-43.

AUTHOR DECLARATIONS

Conflict of Interest

The authors have no conflicts to disclose.

Author Contributions

Linghua Jin: Conceptualization (equal); Data curation (equal); Investigation (equal); Writing – original draft (equal). **Huide Wang:** Project administration (equal); Resources (equal); Writing – review & editing (equal). **Rui Cao:** Resources (equal); Supervision (equal). **Karim Khan:** Writing – review & editing (equal). **Ayesha Khan Tareen:** Project administration (equal). **Swelm Wageh:** Writing – review & editing (equal). **Ahmed A. Al-Ghamdi:** Writing – review & editing (equal). **Shaojuan Li:** Writing – review & editing (equal). **Dabing Li:** Writing – review & editing (equal). **Ye Zhang:** Writing – review & editing (equal). **Han Zhang:** Writing – review & editing (equal).

DATA AVAILABILITY

Data sharing is not applicable to this article as no new data were created or analyzed in this study.

REFERENCES

- A. K. Geim and K. S. Novoselov, *Nat. Mater.* **6**(3), 183–191 (2007).
- K. S. Novoselov, A. K. Geim, S. V. Morozov, D. Jiang, Y. Zhang, S. V. Dubonos, I. V. Grigorieva, and A. A. Firsov, *Science* **306**(5696), 666–669 (2004).
- K. S. Novoselov, V. I. Fal'ko, L. Colombo, P. R. Gellert, M. G. Schwab, and K. Kim, *Nature* **490**(7419), 192–200 (2012).
- L. Li, Y. Yu, G. J. Ye, Q. Ge, X. Ou, H. Wu, D. Feng, X. H. Chen, and Y. Zhang, *Nat. Nanotechnol.* **9**(5), 372–377 (2014).
- K. F. Mak, C. Lee, J. Hone, J. Shan, and T. F. Heinz, *Phys. Rev. Lett.* **105**(13) (2010).
- Q. H. Wang, K. Kalantar-Zadeh, A. Kis, J. N. Coleman, and M. S. Strano, *Nat. Nanotechnol.* **7**(11), 699–712 (2012).
- M. Naguib, V. N. Mochalin, M. W. Barsoum, and Y. Gogotsi, *Adv. Mater.* **26**(7), 992–1005 (2014).
- H. Liu, A. T. Neal, Z. Zhu, Z. Luo, X. Xu, D. Tománek, and P. D. Ye, *Acs Nano* **8**(4), 4033–4041 (2014).
- G. R. Bhimanapati, Z. Lin, V. Meunier, Y. Jung, J. Cha, S. Das, D. Xiao, Y. Son, M. S. Strano, V. R. Cooper, L. Liang, S. G. Louie, E. Ringe, W. Zhou, S. S. Kim, R. R. Naik, B. G. Sumpter, H. Terrones, F. Xia, Y. Wang, J. Zhu, D. Akinwande, N. Alem, J. A. Schuller, R. E. Schaak, M. Terrones, and J. A. Robinson, *Acs Nano* **9**(12), 11509–11539 (2015).
- S. Abdolhosseinzadeh, X. Jiang, H. Zhang, J. Qiu, and C. Zhang, *Mater. Today* **48**, 214–240 (2021).
- D. Y. Qiu, F. H. da Jornada, and S. G. Louie, *Phys. Rev. Lett.* **111**(21), 216805 (2013).
- K. He, N. Kumar, L. Zhao, Z. Wang, K. F. Mak, H. Zhao, and J. Shan, *Phys. Rev. Lett.* **113**(2), 026803 (2014).
- F. Xia, H. Wang, D. Xiao, M. Dubey, and A. Ramasubramaniam, *Nat. Photonics* **8**(12), 899–907 (2014).
- G. Soavi, G. Wang, H. Rostami, D. G. Purdie, D. De Fazio, T. Ma, B. Luo, J. Wang, A. K. Ott, D. Yoon, S. A. Bourelle, J. E. Muench, I. Goykhman, S. Dal Conte, M. Celebrano, A. Tomadin, M. Polini, G. Cerullo, and A. C. Ferrari, *Nat. Nanotechnol.* **13**(7), 583–588 (2018).
- F. Xia, H. Wang, and Y. Jia, *Nat. Commun.* **5**, 4458 (2014).
- X. Wang, Y. Cui, T. Li, M. Lei, J. Li, and Z. Wei, *Adv. Opt. Mater.* **7**(3), 1801274 (2018).
- H. Yuan, X. Liu, F. Afshinmanesh, W. Li, G. Xu, J. Sun, B. Lian, A. G. Curto, G. Ye, Y. Hikita, Z. Shen, S.-C. Zhang, X. Chen, M. Brongersma, H. Y. Hwang, and Y. Cui, *Nat. Nanotechnol.* **10**(8), 707–713 (2015).
- K. F. Mak and J. Shan, *Nat. Photonics* **10**(4), 216–226 (2016).
- H. Mu, S. Lin, Z. Wang, S. Xiao, P. Li, Y. Chen, H. Zhang, H. Bao, S. P. Lau, C. Pan, D. Fan, and Q. Bao, *Adv. Opt. Mater.* **3**(10), 1447–1453 (2015).
- T. Tan, X. Jiang, C. Wang, B. Yao, and H. Zhang, *Adv. Sci.* **7**(11), 2000058 (2020).
- Z.-C. Luo, M. Liu, Z.-N. Guo, X.-F. Jiang, A.-P. Luo, C.-J. Zhao, X.-F. Yu, W.-C. Xu, and H. Zhang, *Opt. Express* **23**(15), 20030–20039 (2015).
- O. Lopez-Sanchez, D. Lembke, M. Kayci, A. Radenovic, and A. Kis, *Nat. Nanotechnol.* **8**(7), 497–501 (2013).
- M. Long, P. Wang, H. Fang, and W. Hu, *Adv. Funct. Mater.* **29**(19), 1803807 (2018).
- Q. Qiu and Z. Huang, *Adv. Mater.* **33**(15), e2008126 (2021).
- N. Huo, S. Yang, Z. Wei, S.-S. Li, J.-B. Xia, and J. Li, *Sci. Rep.* **4**, 5209 (2014).
- Z. Meng, R. M. Stolz, L. Mendecki, and K. A. Mirica, *Chem. Rev.* **119**(1), 478–598 (2019).
- X. Liu, T. Ma, N. Pinna, and J. Zhang, *Adv. Funct. Mater.* **27**(37), 1702168 (2017).
- A. Autere, H. Jussila, Y. Dai, Y. Wang, H. Lipsanen, and Z. Sun, *Adv. Mater.* **30**(24), e1705963 (2018).
- S. Uddin, P. C. Debnath, K. Park, and Y.-W. Song, *Sci. Rep.* **7**, 43371 (2017).
- B. Fu, J. Sun, C. Wang, C. Shang, L. Xu, J. Li, and H. Zhang, *Small* **17**(11), e2006054 (2021).
- L. Cao, H. Chu, H. Pan, R. Wang, Y. Li, S. Zhao, D. Li, H. Zhang, and D. Li, *Opt. Express* **28**(21), 31499–31509 (2020).
- X. Li, Z. Song, H. Zhang, Y. Song, and K. Panajotov, *Front. Phys.* **8**, 632406 (2021).
- J. Fu, M. Qiu, W. Bao, and H. Zhang, *Adv. Electron. Mater.* **7**(7), 2100444 (2021).
- Z. Cheng, R. Cao, K. Wei, Y. Yao, X. Liu, J. Kang, J. Dong, Z. Shi, H. Zhang, and X. Zhang, *Adv. Sci.* **8**(11), e2003834 (2021).
- Y. Shu, J. Guo, T. Fan, Y. Xu, P. Guo, Z. Wang, L. Wu, Y. Ge, Z. Lin, D. Ma, S. Wei, J. Li, H. Zhang, and W. Chen, *ACS Appl. Mater. Interfaces* **12**(41), 46509–46518 (2020).
- A. Hu, H. Tian, Q. Liu, L. Wang, L. Wang, X. He, Y. Luo, and X. Guo, *Adv. Opt. Mater.* **7**(8), 1801792 (2019).
- H. Guan, J. Hong, X. Wang, J. Ming, Z. Zhang, A. Liang, X. Han, J. Dong, W. Qiu, Z. Chen, H. Lu, and H. Zhang, *Adv. Opt. Mater.* **9**(16), 2100245 (2021).
- C. Baeumer, D. Saldana-Greco, J. M. P. Martirez, A. M. Rappe, M. Shim, and L. W. Martin, *Nat. Commun.* **6**, 6136 (2015).
- L. Lv, F. Zhuge, F. Xie, X. Xiong, Q. Zhang, N. Zhang, Y. Huang, and T. Zhai, *Nat. Commun.* **10**(1), 3331 (2019).
- K. K. Gopalan, D. Janner, S. Nanot, R. Parret, M. B. Lundberg, F. H. L. Koppens, and V. Pruneri, *Adv. Opt. Mater.* **5**(4), 1600723 (2017).
- J. Wang, H. Fang, X. Wang, X. Chen, W. Lu, and W. Hu, *Small* **13**(35), 1700894 (2017).
- Y. Y. Hui, X. Liu, W. Jie, N. Y. Chan, J. Hao, Y.-T. Hsu, L.-J. Li, W. Guo, and S. P. Lau, *ACS Nano* **7**(8), 7126–7131 (2013).
- H. Chen, L. Gao, O. A. Al-Hartomy, F. Zhang, A. Al-Ghamdi, J. Guo, Y. Song, Z. Wang, H. Algarni, C. Wang, S. Wageh, S. Xu, and H. Zhang, *Nanoscale* **13**(37), 15891–15898 (2021).
- Y. Sun, G. Niu, W. Ren, X. Meng, J. Zhao, W. Luo, Z. G. Ye, and Y. H. Xie, *ACS Nano* **15**(7), 10982–11013 (2021).
- L. W. Martin and A. M. Rappe, *Nat. Rev. Mater.* **2**(2) (2016).
- L. Jin, F. Li, S. Zhang, and D. J. Green, *J. Am. Ceram. Soc.* **97**(1), 1–27 (2014).
- Editorial, *Nat. Mater.* **19**(2), 129 (2020).
- W.-Q. Liao, Y. Zhang, C.-L. Hu, J.-G. Mao, H.-Y. Ye, P.-F. Li, S. D. Huang, and R.-G. Xiong, *Nat. Commun.* **6**, 7338 (2015).
- G. Catalan and J. F. Scott, *Adv. Mater.* **21**(24), 2463–2485 (2009).
- T. H. Nguyen, V. Q. Nguyen, A. T. Duong, and S. Cho, *J. Alloys Compd.* **810**, 151968 (2019).
- F. Liu, L. You, K. L. Seyler, X. Li, P. Yu, J. Lin, X. Wang, J. Zhou, H. Wang, H. He, S. T. Pantelides, W. Zhou, P. Sharma, X. Xu, P. M. Ajayan, J. Wang, and Z. Liu, *Nat. Commun.* **7**, 12357 (2016).
- M. Osada and T. Sasaki, *APL Mater.* **7**(12), 120902 (2019).
- S. M. Said, M. F. M. Sabri, F. Salleh, and M. Ramadan, *Encycl. Smart Mater.* **3**, 495–506 (2022).
- X. Wang, P. Wang, J. Wang, W. Hu, X. Zhou, N. Guo, H. Huang, S. Sun, H. Shen, T. Lin, M. Tang, L. Liao, A. Jiang, J. Sun, X. Meng, X. Chen, W. Lu, and J. Chu, *Adv. Mater.* **27**(42), 6575–6581 (2015).
- G. Wu, B. Tian, L. Liu, W. Lv, S. Wu, X. Wang, Y. Chen, J. Li, Z. Wang, S. Wu, H. Shen, T. Lin, P. Zhou, Q. Liu, C. Duan, S. Zhang, X. Meng, S. Wu, W. Hu, X. Wang, J. Chu, and J. Wang, *Nat. Electron.* **3**(1), 43–50 (2020).
- G. Wu, X. Wang, Y. Chen, S. Wu, B. Wu, Y. Jiang, H. Shen, T. Lin, Q. Liu, X. Wang, P. Zhou, S. Zhang, W. Hu, X. Meng, J. Chu, and J. Wang, *Adv. Mater.* **32**(16), e1907937 (2020).
- W. Wang, W. Sun, H. Li, Y. Bai, F. Ren, C. You, and Z. Cheng, *Nanoscale* **13**(33), 14214–14220 (2021).
- X. Wang, H. Shen, Y. Chen, G. Wu, P. Wang, H. Xia, T. Lin, P. Zhou, W. Hu, X. Meng, J. Chu, and J. Wang, *Adv. Sci.* **6**(15), 1901050 (2019).
- N. Park, H. Kang, J. Park, Y. Lee, Y. Yun, J.-H. Lee, S.-G. Lee, Y. H. Lee, and D. Suh, *ACS Nano* **9**(11), 10729–10736 (2015).
- C. Ko, Y. Lee, Y. Chen, J. Suh, D. Fu, A. Suslu, S. Lee, J. D. Clarkson, H. S. Choe, S. Tongay, R. Ramesh, and J. Wu, *Adv. Mater.* **28**(15), 2923–2930 (2016).
- Y. Li, X.-Y. Sun, C.-Y. Xu, J. Cao, Z.-Y. Sun, and L. Zhen, *Nanoscale* **10**(48), 23080–23086 (2018).

- ⁶²L. Liu, L. Wu, A. Wang, H. Liu, R. Ma, K. Wu, J. Chen, Z. Zhou, Y. Tian, H. Yang, C. Shen, L. Bao, Z. Qin, S. T. Pantelides, and H.-J. Gao, *Nano Lett.* **20**(9), 6666–6673 (2020).
- ⁶³L. Tu, R. Cao, X. Wang, Y. Chen, S. Wu, F. Wang, Z. Wang, H. Shen, T. Lin, P. Zhou, X. Meng, W. Hu, Q. Liu, J. Wang, M. Liu, and J. Chu, *Nat. Commun.* **11**(1), 101 (2020).
- ⁶⁴D. Wijethunge, C. Tang, C. Zhang, L. Zhang, X. Mao, and A. Du, *Appl. Surf. Sci.* **513**, 145817 (2020).
- ⁶⁵Z. Zhu, X. Chen, W. Li, and J. Qi, *Appl. Phys. Lett.* **114**(22), 223102 (2019).
- ⁶⁶H. Fang and W. Hu, *Adv. Sci.* **4**(12), 1700323 (2017).
- ⁶⁷B. Lin, A. Chaturvedi, J. Di, L. You, C. Lai, R. Duan, J. Zhou, B. Xu, Z. Chen, P. Song, J. Peng, B. Ma, H. Liu, P. Meng, G. Yang, H. Zhang, Z. Liu, and F. Liu, *Nano Energy* **76**, 104972 (2020).
- ⁶⁸U. Sassi, R. Parret, S. Nanot, M. Bruna, S. Borini, D. De Fazio, Z. Zhao, E. Lidorikis, F. H. L. Koppens, A. C. Ferrari, and A. Colli, *Nat. Commun.* **8**, 14311 (2017).
- ⁶⁹A. Chaves, J. G. Azadani, H. Alsalman, D. R. da Costa, R. Frisenda, A. J. Chaves, S. H. Song, Y. D. Kim, D. He, J. Zhou, A. Castellanos-Gomez, F. M. Peeters, Z. Liu, C. L. Hinkle, S.-H. Oh, P. D. Ye, S. J. Koester, Y. H. Lee, P. Avouris, X. Wang, and T. Low, *npj 2D Mater. Appl.* **4**(1), 29 (2020).
- ⁷⁰S. Yang, Y. Chen, and C. Jiang, *InfoMat* **3**(4), 397–420 (2021).
- ⁷¹B. K. Moghal and M. R. Islam, *Mater. Today Commun.* **31**, 103240 (2022).
- ⁷²C. Cui, F. Xue, W.-J. Hu, and L.-J. Li, *npj 2D Mater. Appl.* **2**(1), 18 (2018).
- ⁷³F. Ding, H. Ji, Y. Chen, A. Herklotz, K. Dörr, Y. Mei, A. Rastelli, and O. G. Schmidt, *Nano Lett.* **10**(9), 3453–3458 (2010).
- ⁷⁴W. Jie, Y. Yu Hui, Y. Zhang, S. Ping Lau, and J. Hao, *Appl. Phys. Lett.* **102**(22), 223112 (2013).
- ⁷⁵H.-J. Jin, W. Y. Yoon, and W. Jo, *ACS Appl. Mater. Interfaces* **10**(1), 1334–1339 (2018).
- ⁷⁶X. Liu, X. Yang, G. Gao, Z. Yang, H. Liu, Q. Li, Z. Lou, G. Shen, L. Liao, C. Pan, and Z. Lin Wang, *ACS Nano* **10**(8), 7451–7457 (2016).
- ⁷⁷W. Jie, Y. Y. Hui, N. Y. Chan, Y. Zhang, S. P. Lau, and J. Hao, *J. Phys. Chem. C* **117**(26), 13747–13752 (2013).
- ⁷⁸G.-X. Ni, Y. Zheng, S. Bae, C. Y. Tan, O. Kahya, J. Wu, B. H. Hong, K. Yao, and B. Özyilmaz, *ACS Nano* **6**(5), 3935–3942 (2012).
- ⁷⁹J.-W. Chen, S.-T. Lo, S.-C. Ho, S.-S. Wong, T.-H.-Y. Vu, X.-Q. Zhang, Y.-D. Liu, Y.-Y. Chiou, Y.-X. Chen, J.-C. Yang, Y.-C. Chen, Y.-H. Chu, Y.-H. Lee, C.-J. Chung, T.-M. Chen, C.-H. Chen, and C.-L. Wu, *Nat. Commun.* **9**(1), 3143 (2018).
- ⁸⁰A. Nguyen, P. Sharma, T. Scott, E. Preciado, V. Klee, D. Sun, I.-H. Lu, D. Barroso, S. Kim, V. Y. Shur, A. R. Akhmatkhanov, A. Gruverman, L. Bartels, and P. A. Dowben, *Nano Lett.* **15**(5), 3364–3369 (2015).
- ⁸¹Z. Xiao, J. Song, D. K. Ferry, S. Ducharme, and X. Hong, *Phys. Rev. Lett.* **118**(23), 236801 (2017).
- ⁸²A. Lipatov, T. Li, N. S. Vorobeve, A. Sinitskii, and A. Gruverman, *Nano Lett.* **19**(5), 3194–3198 (2019).
- ⁸³Y. Jeong, H. J. Jin, J. H. Park, Y. Cho, M. Kim, S. Hong, W. Jo, Y. Yi, and S. Im, *Adv. Funct. Mater.* **30**(7), 1908210 (2019).
- ⁸⁴F. Schwierz, *Nat. Nanotechnol.* **5**(7), 487–496 (2010).
- ⁸⁵J. Ding, L. Wen, H. Li, and Y. Zhang, *Phys. Lett. A* **381**(20), 1749–1752 (2017).
- ⁸⁶W. Jie and J. Hao, *Nanoscale* **10**(1), 328–335 (2017).
- ⁸⁷J. Guo, Y. Liu, Y. Lin, Y. Tian, J. Zhang, T. Gong, T. Cheng, W. Huang, and X. Zhang, *Nanoscale* **11**(43), 20868–20875 (2019).
- ⁸⁸H. Wang, H. Zhao, G. Hu, S. Li, H. Su, and J. Zhang, *Sci. Rep.* **5**, 18258 (2015).
- ⁸⁹X. Wang, M. Tang, Y. Chen, G. Wu, H. Huang, X. Zhao, B. Tian, J. Wang, S. Sun, H. Shen, T. Lin, J. Sun, X. Meng, and J. Chu, *Opt. Quantum Electron.* **48**(7), 345 (2016).
- ⁹⁰M. Dragoman, A. Dinescu, F. Nastase, and D. Dragoman, *Nanomaterials* **10**(7), 1404 (2020).
- ⁹¹S. Jung, J. Park, J. Kim, W. Song, J. Jo, H. Park, M. Kong, S. Kang, M. Sheeraz, I. W. Kim, T. H. Kim, and K. Park, *npj 2D Mater. Appl.* **5**(1), 90 (2021).
- ⁹²Z. Li, Y. Zhao, W. Li, Y. Peng, W. Zhao, Z. Wang, L. Shi, and W. Fei, *Mater. Lett.* **305**, 130686 (2021).
- ⁹³D. Kundys, A. Cascales, A. S. Makhort, H. Majjad, F. Chevrier, B. Doudin, A. Fedrizzi, and B. Kundys, *Phys. Rev. Appl.* **13**(6), 064034 (2020).
- ⁹⁴D. T. Debu, F. T. Ladani, D. French, S. J. Bauman, and J. B. Herzog, *npj 2D Mater. Appl.* **3**(1), 30 (2019).
- ⁹⁵M. Zhu, J. Wu, Z. Du, R. Y. Tay, H. Li, B. Özyilmaz, and E. H. T. Teo, *Nanoscale* **7**(35), 14730–14737 (2015).
- ⁹⁶Y. Chen, X. Wang, P. Wang, H. Huang, G. Wu, B. Tian, Z. Hong, Y. Wang, S. Sun, H. Shen, J. Wang, W. Hu, J. Sun, X. Meng, and J. Chu, *ACS Appl. Mater. Interfaces* **8**(47), 32083–32088 (2016).
- ⁹⁷A. Lipatov, P. Sharma, A. Gruverman, and A. Sinitskii, *ACS Nano* **9**(8), 8089–8098 (2015).
- ⁹⁸T. J. Octon, V. K. Nagareddy, S. Russo, M. F. Craciun, and C. D. Wright, *Adv. Opt. Mater.* **4**(11), 1750–1754 (2016).
- ⁹⁹X. Wang, C. Liu, Y. Chen, G. Wu, X. Yan, H. Huang, P. Wang, B. Tian, Z. Hong, Y. Wang, S. Sun, H. Shen, T. Lin, W. Hu, M. Tang, P. Zhou, J. Wang, J. Sun, X. Meng, J. Chu, and Z. Li, *2D Mater.* **4**(2), 025036 (2017).
- ¹⁰⁰D. Li, X. Wang, Y. Chen, S. Zhu, F. Gong, G. Wu, C. Meng, L. Liu, L. Wang, T. Lin, S. Sun, H. Shen, X. Wang, W. Hu, J. Wang, J. Sun, X. Meng, and J. Chu, *Nanotechnology* **29**(10), 105202 (2018).
- ¹⁰¹C. Yin, X. Wang, Y. Chen, D. Li, T. Lin, S. Sun, H. Shen, P. Du, J. Sun, X. Meng, J. Chu, H. F. Wong, C. W. Leung, Z. Wang, and J. Wang, *Nanoscale* **10**(4), 1727–1734 (2018).
- ¹⁰²H. Huang, X. Wang, P. Wang, G. Wu, Y. Chen, C. Meng, L. Liao, J. Wang, W. Hu, H. Shen, T. Lin, J. Sun, X. Meng, X. Chen, and J. Chu, *RSC Adv.* **6**(90), 87416–87421 (2016).
- ¹⁰³Z.-D. Luo, X. Xia, M.-M. Yang, N. R. Wilson, A. Gruverman, and M. Alexe, *ACS Nano* **14**(1), 746–754 (2020).
- ¹⁰⁴X. Liu, R. Liang, G. Gao, C. Pan, C. Jiang, Q. Xu, J. Luo, X. Zou, Z. Yang, L. Liao, and Z. L. Wang, *Adv. Mater.* **30**(28), e1800932 (2018).
- ¹⁰⁵X. Wang, Y. Chen, G. Wu, D. Li, L. Tu, S. Sun, H. Shen, T. Lin, Y. Xiao, M. Tang, W. Hu, L. Liao, P. Zhou, J. Sun, X. Meng, J. Chu, and J. Wang, *npj 2D Mater. Appl.* **1**(1), 38 (2017).
- ¹⁰⁶M. Si, C.-J. Su, C. Jiang, N. J. Conrad, H. Zhou, K. D. Maize, G. Qiu, C.-T. Wu, A. Shakouri, M. A. Alam, and P. D. Ye, *Nat. Nanotechnol.* **13**(1), 24–28 (2018).
- ¹⁰⁷Z. Luo, Z. Wang, Z. Guan, C. Ma, L. Zhao, C. Liu, H. Sun, H. Wang, Y. Lin, X. Jin, Y. Yin, and X. Li, *Nat. Commun.* **13**(1), 699 (2022).
- ¹⁰⁸S. Oh, H. Hwang, and I. K. Yoo, *APL Mater.* **7**(9), 091109 (2019).
- ¹⁰⁹Y. Zhou, Y. Wang, F. Zhuge, J. Guo, S. Ma, J. Wang, Z. Tang, Y. Li, X. Miao, Y. He, and Y. Chai, *Adv. Mater.* (published online 2022).
- ¹¹⁰Y. T. Lee, H. Kwon, J. S. Kim, H.-H. Kim, Y. J. Lee, J. A. Lim, Y.-W. Song, Y. Yi, W.-K. Choi, D. K. Hwang, and S. Im, *ACS Nano* **9**(10), 10394–10401 (2015).
- ¹¹¹Y. T. Lee, D. K. Hwang, and W. K. Choi, *J. Korean Phys. Soc.* **69**(8), 1347–1351 (2016).
- ¹¹²S. Yan, H. Huang, Z. Xie, G. Ye, X.-X. Li, T. Taniguchi, K. Watanabe, Z. Han, X. Chen, J. Wang, and J.-H. Chen, *ACS Appl. Mater. Interfaces* **11**(45), 42358–42364 (2019).
- ¹¹³L. Xie, X. Chen, Z. Dong, Q. Yu, X. Zhao, G. Yuan, Z. Zeng, Y. Wang, and K. Zhang, *Adv. Electron. Mater.* **5**(8), 1900458 (2019).
- ¹¹⁴J. M. Yan, J. S. Ying, M. Y. Yan, Z. C. Wang, S. S. Li, T. W. Chen, G. Y. Gao, F. Liao, H. S. Luo, T. Zhang, Y. Chai, and R. K. Zheng, *Adv. Funct. Mater.* **31**(40), 2103982 (2021).
- ¹¹⁵M. Wu, *ACS Nano* **15**(6), 9229–9237 (2021).
- ¹¹⁶Z. Guan, H. Hu, X. Shen, P. Xiang, N. Zhong, J. Chu, and C. Duan, *Adv. Electron. Mater.* **6**(1), 1900818 (2019).
- ¹¹⁷M. Wu and P. Jena, *WIREs Comput. Mol. Sci.* **8**(5), e1391 (2018).
- ¹¹⁸K. Xu, W. Jiang, X. Gao, Z. Zhao, T. Low, and W. Zhu, *Nanoscale* **12**(46), 23488–23496 (2020).
- ¹¹⁹M. Liu, T. Liao, Z. Sun, Y. Gu, and L. Kou, *Phys. Chem. Chem. Phys.* **23**(38), 21376–21384 (2021).
- ¹²⁰D. Dutta, S. Mukherjee, M. Uzhansky, and E. Koren, *npj 2D Mater. Appl.* **5**(1), 81 (2021).
- ¹²¹L. Qi, S. Ruan, and Y. J. Zeng, *Adv. Mater.* **33**(13), e2005098 (2021).
- ¹²²K. S. Novoselov, A. Mishchenko, A. Carvalho, and A. H. Castro Neto, *Science* **353**(6298), aac9439 (2016).
- ¹²³P. V. Pham, S. C. Bodepudi, K. Shehzad, Y. Liu, Y. Xu, B. Yu, and X. Duan, *Chem. Rev.* **122**(6), 6514–6613 (2022).

- ¹²⁴X. Wang, P. Yu, Z. Lei, C. Zhu, X. Cao, F. Liu, L. You, Q. Zeng, Y. Deng, C. Zhu, J. Zhou, Q. Fu, J. Wang, Y. Huang, and Z. Liu, *Nat. Commun.* **10**(1), 3037 (2019).
- ¹²⁵W. Huang, F. Wang, L. Yin, R. Cheng, Z. Wang, M. G. Sendeku, J. Wang, N. Li, Y. Yao, and J. He, *Adv. Mater.* **32**(14), e1908040 (2020).
- ¹²⁶B. Zhou, S.-J. Gong, K. Jiang, L. Xu, L. Zhu, L. Shang, Y. Li, Z. Hu, and J. Chu, *J. Phys.: Condens. Matter* **32**(5), 055703 (2020).
- ¹²⁷X. Duan, S. Tang, and Z. Huang, *Comput. Mater. Sci.* **200**, 110819 (2021).
- ¹²⁸X. Mao, J. Fu, C. Chen, Y. Li, H. Liu, M. Gong, and H. Zeng, *ACS Appl. Mater. Interfaces* **13**(20), 24250–24257 (2021).
- ¹²⁹X. Wang, C. Zhu, Y. Deng, R. Duan, J. Chen, Q. Zeng, J. Zhou, Q. Fu, L. You, S. Liu, J. H. Edgar, P. Yu, and Z. Liu, *Nat. Commun.* **12**(1), 1109 (2021).
- ¹³⁰F. Guo, M. L. Song, M. C. Wong, R. Ding, W. F. Io, S. Y. Pang, W. J. Jie, and J. H. Hao, *Adv. Funct. Mater.* **32**(6), 2108014 (2022).
- ¹³¹P. Li, A. Chaturvedi, H. Zhou, G. Zhang, Q. Li, J. Xue, Z. Zhou, S. Wang, K. Zhou, Y. Weng, F. Zheng, Z. Shi, E. H. T. Teo, L. Fang, and L. You, *Adv. Funct. Mater.* (published online 2022).